IEEE Photonics Journal
An IEEE Photonics Society Publication

Noise Reduction in Digital Hologram Using Wavelet Transforms and Smooth Filter for Three-Dimensional Display

Volume 5, Number 3, June 2013

Le Thanh Bang
Weina Li
Mei-Lan Piao
Md. Ashraful Alam
Nam Kim

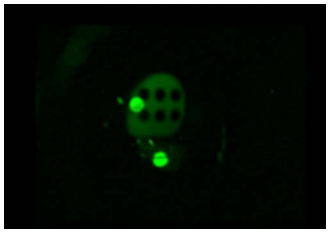

DOI: 10.1109/JPHOT.2013.2265979
1943-0655/$31.00 ©2013 IEEE

Noise Reduction in Digital Hologram Using Wavelet Transforms and Smooth Filter for Three-Dimensional Display

Le Thanh Bang, Weina Li, Mei-Lan Piao, Md. Ashraful Alam, and Nam Kim

School of Electrical and Computer Engineering, Chungbuk National University, Cheongju 361-763, Korea

DOI: 10.1109/JPHOT.2013.2265979
1943-0655/$31.00 ©2013 IEEE

Manuscript received March 28, 2013; revised May 16, 2013; accepted May 24, 2013. Date of publication June 6, 2013; date of current version June 19, 2013. This work was supported in part by the National Research Foundation of Korea (NRF) grant funded by the Korea government (MEST) under Grant 2012-0030815 and in part by the IT R&D program of MKE/KEIT under Grant KI001810039169 (Development of Core Technologies of Holographic 3D Video System for Acquisition and Reconstruction of 3D Information). Corresponding author: N. Kim (e-mail: namkim@chungbuk.ac.kr).

Abstract: A noise reduction method of Fresnel computer-generated hologram (CGH) using wavelet transform and smooth filter is presented. Noise in hologram is very difficult to remove because an interference pattern is recorded on a digital camera during the digital processing. It also occurs in the reconstruction process, which is affected by discrete quantizing levels and optical experiment setup. So, we develop an algorithm that is capable of changing pixel values at different scales with imaginary or real value according to the requirements of each position in the hologram. A new algorithm is proposed to satisfy the above requirements using a mathematical transformation between the smooth filter function and mother wavelet function in a wavelet transform. In this paper, a theoretical model to predict the effect of noise is described and verified by the experimental results. Based on this, the resultant noises in the reconstructed image by Fresnel CGH algorithm are decreased clearly when spatial light modulator (SLM) for 3D object is placed at distance from 260 mm to 900 mm. The enhanced 3D images can be obtained from digital holograms using efficient noise reduction algorithm to apply this proposed model.

Index Terms: Holographic display, digital holography, spatial light modulator, phase modulation, image recognition, wavelet transform.

1. Introduction

Digital holographic displays use the diffraction effect from a recording medium to reconstruct the 3D objects. It is an advanced technology that can replay 3D objects with full color and wide depth cues, without using any glasses [1]. However, the reconstruction image from the hologram contains heavy obstacles due to white noise and speckle noise [2]. To solve this problem, we need proper filter algorithm and clearly experimental setup when replaying the hologram.

There are several reasons to derive noise in the processing of digital hologram [2], [3]. Generally, the noise comes from three main sources. First, it is related to the optical components, which make multiple interference fringes on the recording plane [4]. Secondly, it comes from the process of set up of the experiment [5]. Because the hologram setup requires a low concentration of the particles [3], which create a spotted diffraction pattern in the CCD camera. With many particles, several diffraction patterns are superimposed and make speckle noise that disturbs the reconstruction of the particle object. Therefore, speckle noise and white noise will appear when the phase or intensity

of the object beam and reference beam is different. Thirdly, digital holograms are captured using a physical system as opposed to an idealized system in computer-generated holography, so there is a lot of wrong information included in the hologram. On the other hand, approximation pixel values by a Fresnel or Fourier transform in the CGH algorithm also produces false signal in the reconstruction of 3D objects [6].

One holographic setup method that can reduce the noises mostly is a wider viewing angle from conventional digital hologram using an off-axis configuration, called phase-shifting digital holography [7]. Using a filter algorithm, one can reduce the noise of a hologram reconstruction [10]–[12]. A quantization algorithm has been applied successfully to holographic data for amplitude and phase quantization [10], [12]. Uniform quantization was implemented as an extremely fast and simple technique [13], [14]. Non-uniform quantization reduces more noise, but it is time-consuming due to its iterative nature, so this method does not remove the high frequency interference and speckle noise. The histogram quantization technique [13], like uniform quantization, requires just one pass through the pixel values but shows the improved results of non-uniform quantization. They combine pixel values between the cluster center from histogram plots of real and imaginary digital hologram. Some communication theories are known as optimal signal quantization under very specific conditions (scalar quantization, a specific error metric, and real valued 1-D signals) and have been used to create a new algorithm that progresses in reducing and removing white noise as Max's algorithm [15], called the Lloyd–Max algorithm [16] but with no significant reduction in white noise and speckle noise.

However, some previous researches had reduced white noise and speckle noise by using image processing [2], [8], [9] or transformation [8], [17]. In these studies, to remove the noise, a filtering scheme is needed that can decompose holograms at different scales and then remove the wrong pixel values variations as in [18]. From these previous studies, to achieve good results for reducing noise in the holographic process, the algorithm should have two characteristics. First, it should be a differential operator to change valued pixels at different scales according to the requirements of each position in the hologram. Secondly, it should be capable of being tuned to act at any desired scale. So, we propose a new algorithm using a mathematical transformation between the smooth filter function and mother wavelet function in wavelet transform to be able to satisfy both of the above conditions.

In this paper, wavelet smooth filter [17] and Taylor smooth filter [19], [20] have been used. Results from previous research by using quantization methods [10], [11], [13] and conventional CGH reconstruction were compared with the results of the proposed method. Normal root mean square (NRMS) parameter is also used to assess the quality of the hologram reconstruction.

Three-dimensional (3-D) objects are captured using phase-shift digital holography and smooth filter and are described in Session II and Session III. The entire process of transforming mathematics for noise-reducing holograms and the simulation in MATLAB are described in Session IV. The results of using the proposed method for noise-reducing of hologram reconstruction are shown in Session V and conclude in Session VI.

2. Phase-Shifting Digital Holography

In [21], the hologram field and the object field are related by the Fresnel diffraction integral

$$U_h(x,y) = e^{j\frac{\pi}{\lambda z}(x^2+y^2)} \int_{\infty}^{\infty}\int U_0(\zeta,\eta) e^{j\frac{\pi}{\lambda z}(\zeta^2+\eta^2)} \exp\left[-j\frac{2\pi}{\lambda z}(x\zeta+yn)\right] d\zeta\, d\eta \tag{1}$$

where $U_h(x,y)$ is the complex amplitude of the diffraction pattern of hologram, $U_0(\zeta,\eta)$ is the intensity of the optically-recorded hologram, x, y is the position of pixels in the hologram plane, ζ,η is the position of pixels in the camera plane, and z is the distance between hologram plane and object plane.

Fig. 1 shows a method for recording hologram known as *phase-shifting* interferometry (PSI) [7]; it simplified the recording setup and the reconstruction of the objects. A laser beam of wavelength

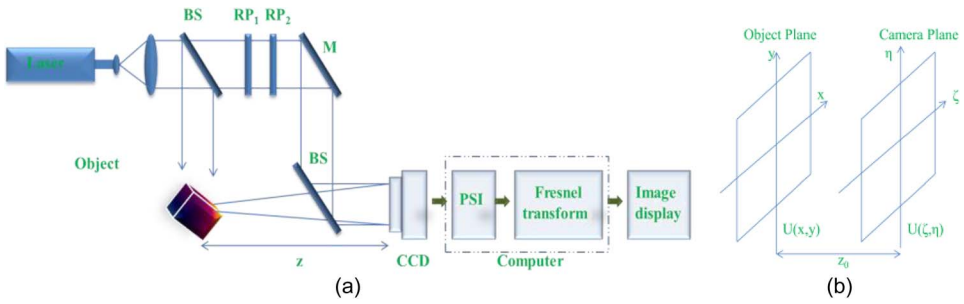

Fig. 1. (a) Experiment setup for phase-shifting hologram; BS: beam splitter, RP: retardation plate, M: mirror. (b) Coordinate for hologram reconstruction.

$\lambda = 532$ nm is divided by a beam splitter into two paths. The object beam is reflected from object to CCD, which is located at distance d from 350 mm to 900 mm from the CCD camera. The other path is a reference beam, which passes through the half-wave plate RP_1 and quarter-wave plate RP_2. This beam can be phase-modulated by rotating the two retardation plates. Four interference patterns $H(x, y, \varphi)$ corresponding to the phase-shift step of $\varphi = 0$, $(\pi/2)$, π and $(3\pi)/2$ are captured by a CCD camera. Using the four step PSI algorithm [7], [22], the wavefront at the plane of the camera can be calculated as follows:

$$H(x,y) = \frac{1}{A_r}\left\{[I(x,y;0) - I(x,y;\pi)] + i\left[I\left(x,y;\frac{\pi}{2}\right) - I\left(x,y;\frac{3\pi}{2}\right)\right]\right\}. \tag{2}$$

A digital hologram $H(x, y)$ contains sufficient amplitude and phase information to reconstruct the complex field $U(x, y, z)$ in the object plane by an object beam at any distance z from CCD [7], [23] using the Fresnel approximation [21] as follows:

$$U(x,y,z) = -\frac{i}{\lambda z}\exp\left(i\frac{2\pi}{\lambda}z\right)H(x,y) * \exp\left[\frac{i\pi}{\lambda z}x^2 + y^2\right] \tag{3}$$

where λ is the wavelength of the illumination, $*$ denotes a convolution operator, z is the distance from the hologram plane to the object plane, and z must be satisfied the condition:

$$z^3 \gg \frac{\pi}{4\lambda}\left[(x-\zeta)^2 + (y-\eta)^2\right]. \tag{4}$$

In this paper, a screw, cubic objects approximately $2 \times 7 \times 2$ mm, $5 \times 5 \times 5$ mm are positioned 350 mm to 900 mm from the CCD camera.

3. Proposed Method

A removal of the noise hologram can be accomplished by various methods; each method has different effectiveness. A best method for removing high frequency use low-pass filter [17]. While use a quantization method [22] such as a histogram quantization, a uniform quantization is the best for reducing speckle noise and white noise in hologram reconstruction process. A general process of hologram noise reduction is shown in Fig. 2. First, hologram data pass through a transformation to series of coefficients. These coefficients are continuous to be filtered or quantized to remove the noise [13], [14], [17]. This data stream is reconstructed 3D object.

Fig. 3 shows the block diagram of the proposed method. In this system, we introduce a new algorithm for noise reduction of the amplitude and phase hologram using smooth filter (see Fig. 4) with the wavelet transform. This system can be capable of changing at different sizes of filter construction so it can flexible to change the pixel value of each fringe on hologram, so this method is very efficient in filtering the pixel values i.e., reducing the data noise that appear in reconstructed hologram. The proposed method is performed by the following steps.

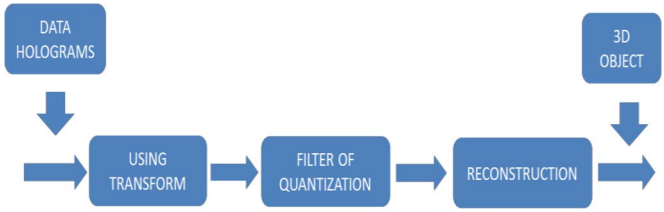

Fig. 2. Diagram of reducing noise hologram.

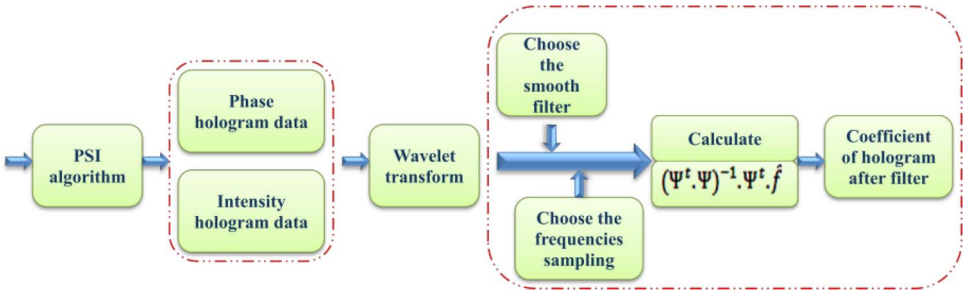

Fig. 3. Proposed algorithm for noise-reducing hologram.

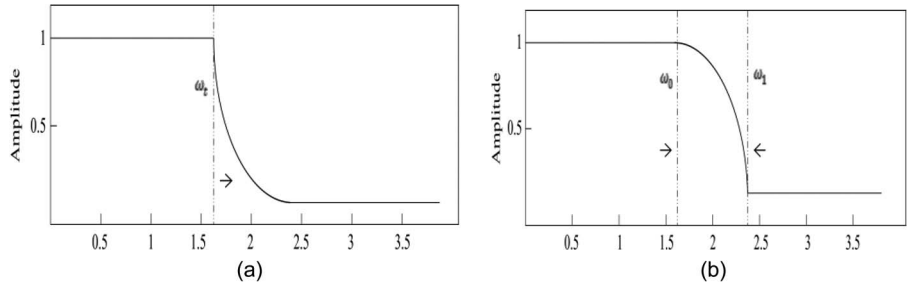

Fig. 4. (a) Wavelet smooth filter. (b) Taylor-series cosine smooth filter.

First step: A hologram is recorded by CCD using an optical system shown in Fig. 1 with four phases that are 0, $\pi/2$, π, and $(3\pi)/2$. These holograms are used to calculate the phase and amplitude holograms by a PSI [7] algorithm.

Second step: Choosing a smooth filter that can be flexible in choosing the frequency filter for low-pass and high-pass filters. In this paper, the wavelet smooth filter and the Taylor-series cosine smooth filter, was applied. Two filters are described in Section 3.1. In this step, choosing the sampling n of function smooth filter to reduce the computational efficiency is also important issue; it is described detail in Section 3.3.

Third step:

In this step, we perform two processes.

- Finding parameter v_i. It is described detail in Section 3.1.
- Implementing the multiplication between the parameter v_i and the wavelet coefficients of hologram $C(x, s_i)$.

This step is described by mathematics as follows.

Hologram data from first step are complex holograms including phase hologram and amplitude hologram. Assume that the filter function that we choose in second step used for a hologram has coefficient as follows:

$$f = f(x_1), f(x_2), \ldots, f(x_n). \tag{5}$$

Therefore, the pixel value of a hologram after using the filter function is given by

$$H_f(x) = \sum_{k=0}^{N-1} f(x_k) H(x_k) \tag{6}$$

where $H(x_k)$ is the pixel value of hologram, and $f(x_k)$ is the value of filter function.

Continuous wavelet transform (CWT) is represented by the following equation:

$$C(x, s) = H(x) * \psi^*\left(\frac{x}{s}\right) \tag{7}$$

where $H(x)$ is hologram data, $\psi(x)$ is the mother function, and $C(x, s)$ is the wavelet coefficients with s as a scale parameter.

Using Fourier transform, Eq. (7) becomes

$$\hat{C}(\omega, s) = \widehat{H}(\omega).\widehat{\psi}^*(s.\omega). \tag{8}$$

A wavelet-based transform filter generations that are able to respond the changes of the hologram pixel values are described. First, we multiply the wavelet coefficients of the hologram with a vector **V** where $v_i = v(s_i)$, and from Eq. (8), we have

$$\sum_{i=0}^{n-1} v_i \hat{C}(\omega, s_i) = \sum_{i=0}^{n-1} v_i \widehat{H}(\omega).\widehat{\psi}^*(s_i\omega)$$

or

$$\sum_{i=0}^{n-1} v_i \widehat{\psi}^*(s_i\omega)\widehat{H}(\omega) = \sum_{I=0}^{n-1} v_i \hat{C}(\omega, s_i). \tag{9}$$

Now, $\hat{f}(\omega)$ can be defined by

$$\hat{f}(\omega) = \sum_{i=0}^{n-1} v_i \widehat{\psi}^*(s_i\omega). \tag{10}$$

Then

$$\hat{f}(\omega).\hat{H}(\omega) = \sum_{i=0}^{n-1} v_i.\hat{C}(\omega, s_i). \tag{11}$$

With an inverse Fourier transform of Eq. (11), then

$$H_f(x) = f(x) * H(x) = \sum_{j=0}^{n-1} v_i C(x, s_i). \tag{12}$$

From Eq. (6) and Eq. (12), it can be found that $f(x)$ is the filter function, $H_f(x)$ is the coefficient of the hologram after using filter function $f(x)$, and in the right side of Eq. (12), we also see that $H_f(x)$ depends on two parameters: the wavelet coefficient of hologram $C(x, s_i)$ and the parameter v_i. So, the value $H_f(x)$ can be capable of changing at different scales s_i and function v_i according to the requirements of each position in the hologram.

Fourth step: The results of two processes that performed in third step are the coefficient of hologram as a usual wavelet coefficient. And then, an inverse wavelet transform is applied to get the noise reduced new hologram. This hologram is reconstructed by CGH (Computer General Hologram) algorithm or spatial light modulator (SLM) devices. In our experiment, firstly, we show some results by reconstructing cubic object and screw object by CGH algorithm; after that, we reconstruct object with Holoeye SLM.

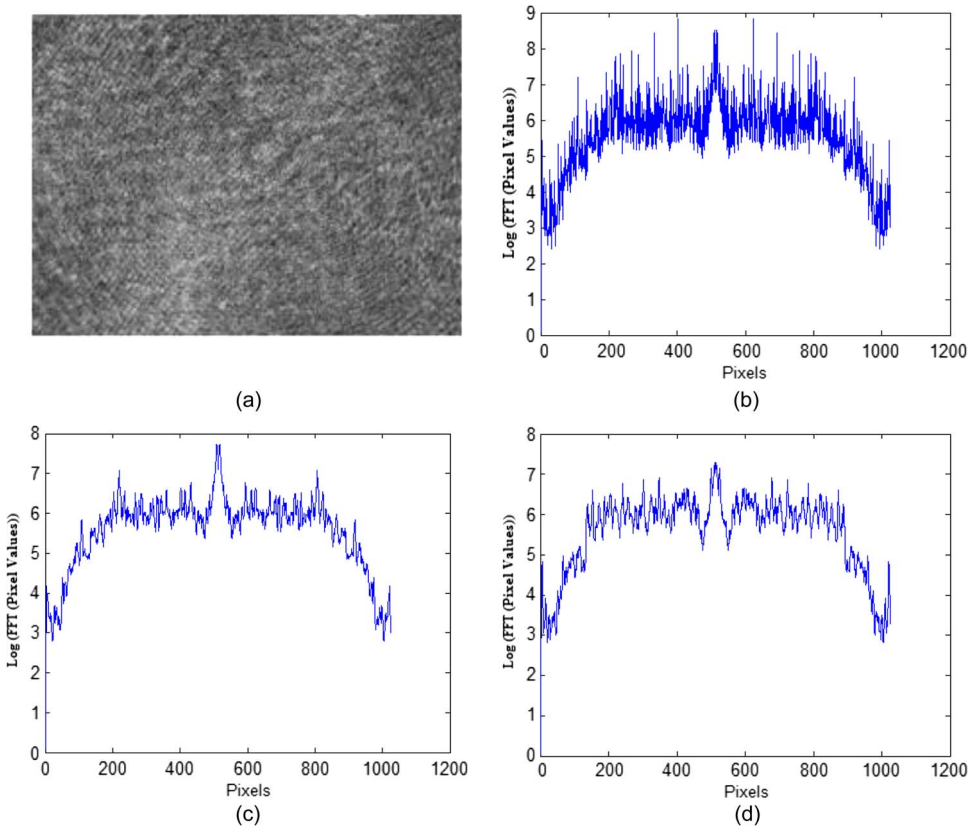

Fig. 5. (a) Hologram of cubic object with z = 550 mm, (b) pixel values from 51th line of hologram after log (FFT(H(51,y)))—FFT(Fast Fourier Transform), (c) using wavelet smooth filter, (d) using Taylor-series cosine smooth filter.

3.1. Choosing Smooth Filter

Among several algorithm of noise reduction of digital hologram, some low-pass filter is applied [17], [18], [28]. In this paper, two smooth filters, which are the wavelet smooth filter [24] and Taylor-series cosine smooth filter [26], are described in Fig. 5 and selected for the proposed algorithm.

In wavelet smooth filter [24], beside depending on the filter frequency, a frequency passes also depends on the distance from CCD to object of the hologram. Therefore, we can assess the quality of the reconstruction Fresnel hologram at different distances. The wavelet smooth filter is described as follows:

$$\hat{f}(\omega_r) = \begin{cases} 1 & \omega_r \leq \omega_t \\ e^{-z*(\omega_r - \omega_t)} & \omega_r > \omega_t \end{cases} \tag{13}$$

where ω_t is the frequency that we chose for the filter, and z is the distance from object and CCD.

As the hologram is generated by the interference of object wave and reference wave, so the fringes appear at different position of hologram. Therefore, a filter that can have a flexible change specified frequency at different position is necessary for checking effect of the proposed algorithm. The Taylor-series smooth filer [26] has met these requirements; it is given as

$$\hat{f}(\omega_r) = \begin{cases} 1 & \omega_r \leq \omega_0 \\ \cos\left[\frac{\pi}{2}\frac{\omega_1 - \omega_r}{\omega_1 - \omega_0}\right] & \omega_0 \leq \omega_r \leq \omega_1 \\ 0 & \omega_r \geq \omega_1 \end{cases} \tag{14}$$

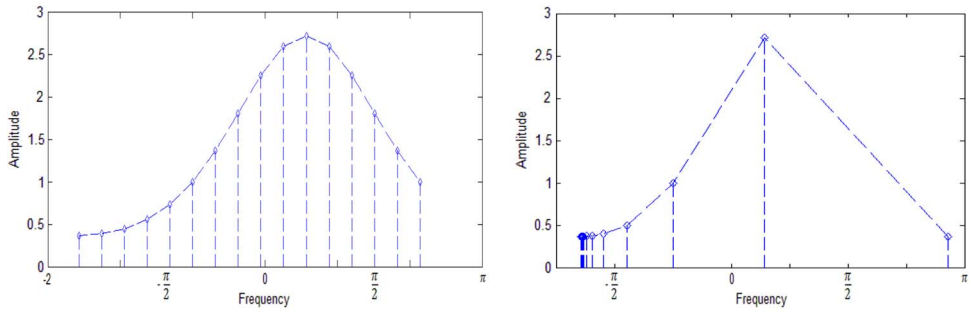

Fig. 6. Sampling of frequency with (a) equally spaced frequency method, (b) exponential frequency method.

where $\omega_0 = 1/(1.5z + (n+1)\delta)$, and $\omega_1 = 1/(z + n\delta)$, with z is the distance from CCD to the object, δ is the size of a small block, and n is the filter order 1, 2, or 3.

3.2. Finding the Parameter v_i

Now, the goal is to find v_i with different filter functions $f(x)$. Recall from Eq. (10) that

$$\hat{f} = V.\Psi$$

where

$$\Psi = [\widehat{\psi^*}(s_0\mathbf{w}) \quad \widehat{\psi^*}(s_1\mathbf{w}) \quad \widehat{\psi^*}(s_2\mathbf{w}) \ldots\ldots\ldots\ldots\ldots\ldots \widehat{\psi^*}(s_{k-2}\mathbf{w})\widehat{\psi^*}(s_{k-1}\mathbf{w}) \tag{15}$$

is matrix $n \times k$ with $\mathbf{w} = (\omega_0\ \omega_1\ \omega_2 \ldots\ldots \omega_{n-2}\ \omega_{n-1})^t$ as follows:

$$\Psi = \begin{bmatrix} \widehat{\psi^*}(s_0\omega_0) & \widehat{\psi^*}(s_1\omega_0) & \widehat{\psi^*}(s_2\omega_0) \ldots\ldots\ldots\ldots\ldots\ldots \widehat{\psi^*}(s_{k-2}\omega_0) & \widehat{\psi^*}(s_{k-1}\omega_0) \\ \widehat{\psi^*}(s_0\omega 1) & \widehat{\psi^*}(s_1\omega 1) & \widehat{\psi^*}(s_2\omega 1) \ldots\ldots\ldots\ldots\ldots\ldots \widehat{\psi^*}(s_{k-2}\omega 1) & \widehat{\psi^*}(s_{k-1}\omega 1) \\ \cdots & \cdots & \cdots \quad \cdots & \ldots\ldots \\ \cdots & \cdots & \cdots \quad \cdots & \ldots\ldots \\ \cdots & \cdots & \cdots \quad \cdots & \ldots\ldots \\ \widehat{\psi^*}(s_0\omega_{n-1}) & \widehat{\psi^*}(s_1\omega_{n-1}) & \widehat{\psi^*}(s_2\omega_{n-1}) \ldots\ldots\ldots\ldots\ldots\ldots \widehat{\psi^*}(s_{k-2}\omega_{n-1}) & \widehat{\psi^*}(s_{k-1}\omega_{n-1}) \end{bmatrix}$$

$V = (v_0\ v_1\ v_2 \ldots\ldots v_{n-2}v_{n-1})^t$ and $\hat{f} = (\hat{f}(\omega_0)\ \hat{f}(\omega_1)\ \hat{f}(\omega_2) \ldots\ldots\ldots\ldots \hat{f}(\omega_{n-2})\ \hat{f}(\omega_{n-1}))$.

Therefore

$$\Psi^t.\hat{f} = V.\Psi^t.\Psi \Leftrightarrow V = (\Psi^t.\Psi)^{-1}.\Psi^t.\hat{f}. \tag{16}$$

So from the Fourier transform of filter function f and the mother function of the wavelet transform, the parameter V can be calculated.

3.3. Finding the Sampling n

From Eq. (10) and Eq. (16), to reduce the computational efficiency and the pixel values in each scale filter construction, the sampling n and the scales k should be calculated precisely, in order to make the condition number of matrix $\Psi(\omega_n, s_k)$ not significantly change [27].

There are two sampling methods to choose the value of n. First is sampling with each frequency equally spaced as Fig. 6(a) that frequencies are chosen

$$\omega_j = \omega_0 + j\Delta\omega \quad \text{with} \quad \Delta\omega = \frac{\omega_{n-1} - \omega_0}{n-1}. \tag{17}$$

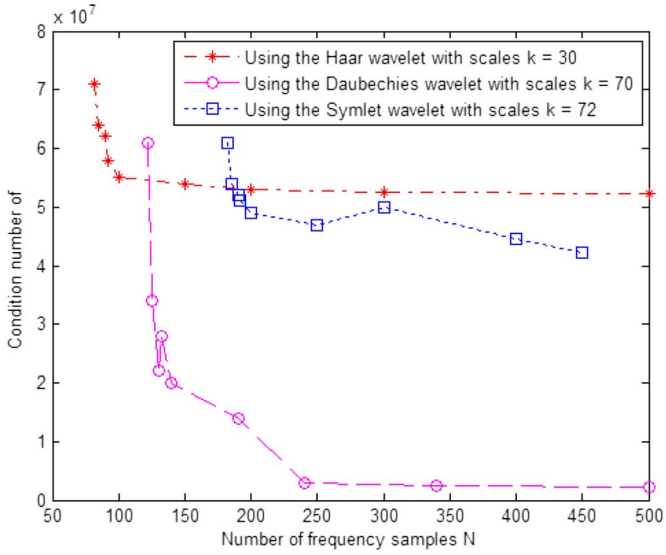

Fig. 7. Dependence of the condition number of Ψ_t. Ψ according to the frequency samples n.

Alternatively, frequencies are chosen using an exponential to define the frequencies as Fig. 6(b)

$$\omega_j = \omega_0 2^{j/p} \tag{18}$$

where

$$p = \frac{n-1}{\log_2[\omega_n - 1] - \log_2[\omega_0]}. \tag{19}$$

The choice of the number of frequencies n in the sampling affects both the stability and the efficiency. The condition number of matrix Ψ for the Haar wavelet with $k = 30$, Daubechies wavelet with $k = 70$, and Symlet wavelet with $k = 72$ are plotted as shown in Fig. 7. With the Haar wavelet, the best choice is above $n = 200$. With the Daubechies wavelet, the best choice is above $n = 242$, and with Symlet wavelet, the best choice is above $n = 450$. Increasing n above those values does not significantly change the condition number of $\Psi_t.\Psi$ but reduces the computational efficiency of the scale filter construction.

4. Experimental Results

There are two parameters that used to evaluate the reduced noise of this hologram, i.e., NRMS [14] and speckle index [30]. The speckle index is the ratio of standard deviation to mean of intensity in a homogeneous area of an object [28]–[30]. A small $a \times a$ pixel block of each hologram is used to calculate this speckle index. Let $p(m, n)$, $1 \leq n \leq N$, and $1 \leq m \leq M$ be the pixel values of small block. The local deviation of pixel values

$$\sigma(m, n) = \max(p(m + i, n + j)) - \min(p(m + i, n + j)) \tag{20}$$

where $0 \leq i \leq a - 1$, and $0 \leq j \leq a - 1$.

And the local mean pixel values in the small block are defined as

$$\mu(m, n) = \frac{1}{a * a} \sum_{i,j=0}^{a-1} p(m + i, n + j). \tag{21}$$

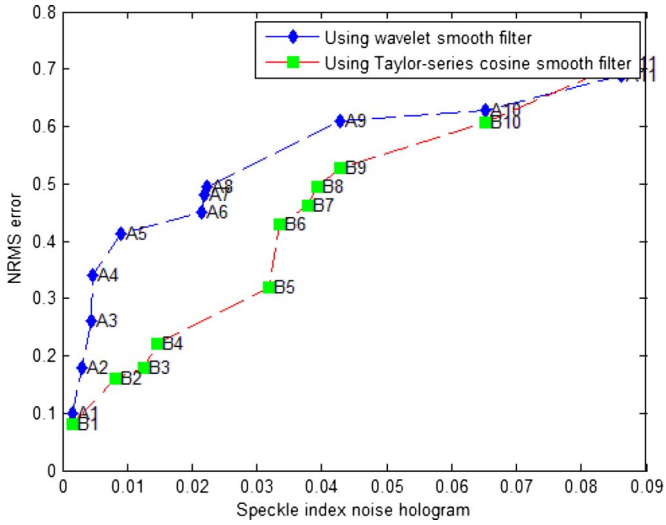

Fig. 8. NRMS error of the hologram reconstruction process and speckle index noise of hologram.

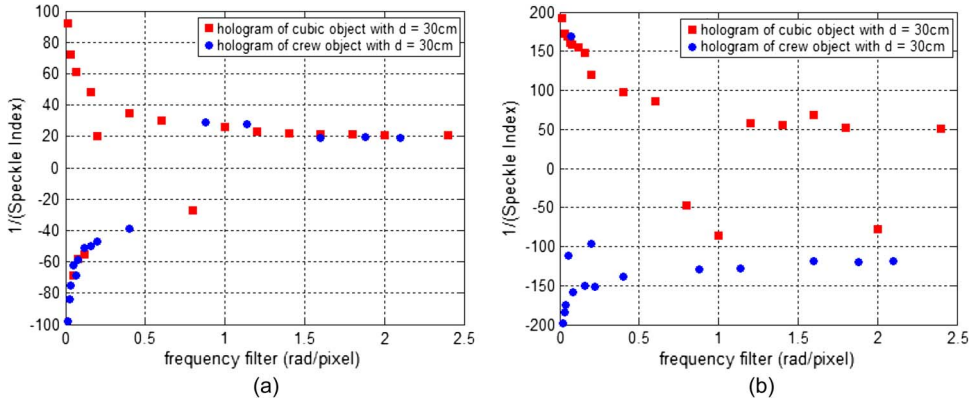

Fig. 9. (a) Speckle index noise when we change ω_t of wavelet smooth filter. (b) Speckle noise index when we change ω_0 and ω_1 of Taylor-series cosine smooth filter.

Finally, the speckle index is defined as

$$S = \frac{1}{(N-2)*(M-2)} \sum_{m,n=1}^{M-2,N-2} \frac{\sigma(m,n)}{\mu(m,n)}. \tag{22}$$

Experiments have been done with laser beam of wave length $\lambda = 532$ nm, CCD camera of resolution 1024 $\times$ 768 pixels with pixel size 9 μm $\times$ 9 μm, and SLM of resolution 1920 $\times$ 1080 pixels with pixel size 8 μm $\times$ 8 μm.

In the proposed method, speckle noise depends on four factors, i.e., the sampling frequencies of filter function, the filter parameter ω, size of block in sub-band σ, and different distances from object plane and camera plane. The effects of these four factors are shown in Figs. 8 –11.

In Fig. 8, we compared the speckle index change of noise hologram when applying our proposed method with a Taylor-series cosine smooth filter and a wavelet smooth filter, with NRMS error in the hologram reconstruction process. From Fig. 8, the speckle index noise and NRMS errors are relatively linear. The points B_1, B_2, B_3, B_4, B_5, and B_6 use Symlet wavelet mother with scale $k = 72$ and sampling frequencies of filter function $n = 210$, filter frequency $\omega_0 = 0.8$ $\omega_1 = 1.9$, size of small block change 2 $\times$ 2, 4 $\times$ 4, and 8 $\times$ 8, and filter order $n = 2, 3$, respectively. For points B_7, B_8, B_9,

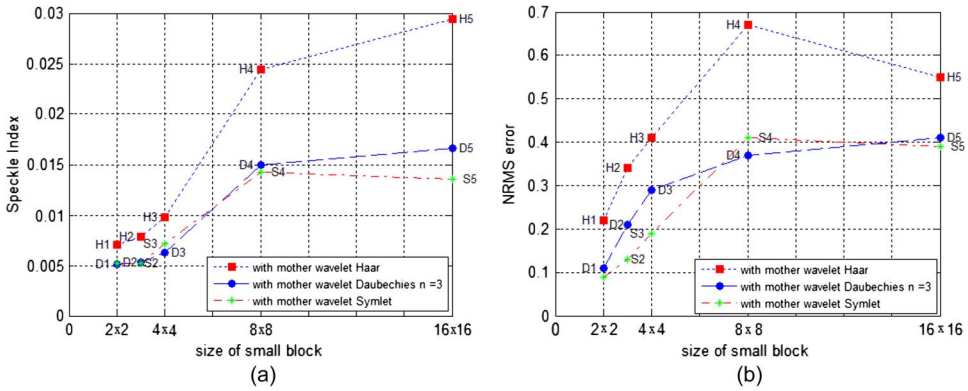

Fig. 10. (a) Speckle index noise. (b) NRMS error when we change parameter size of small block in Taylor-series cosine smooth filter with mother wavelet transform.

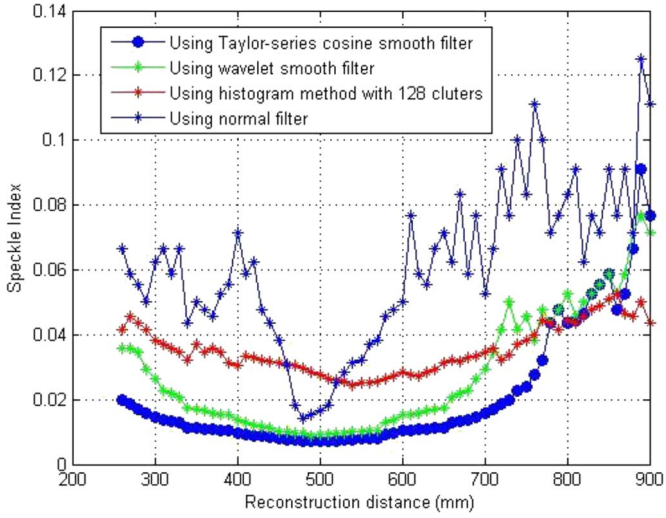

Fig. 11. Speckle index of the object reconstruction at different distances.

B_{10}, and B_{11}, we use Daubechies wavelet mother function with scale $k = 70$ and $n = 3$, sampling frequencies of filter function $n = 210$, filter frequency $\omega_0 = 0.6$ $\omega_1 = 1.1$ 1.7 and 2.2, respectively, size of small block change 2×2, 4×4, and 8×8, and filter order $n = 2, 3$. In this case, a hologram of all points has been recorded by cubic object and distance between CCD and the object that is 550 mm. Similarly, A_1, A_2, A_3, A_4, A_5, and A_6 have a parameter similar as B_1, B_2, B_3, B_4, B_5, and B_6; A_7, A_8, A_9, A_{10}, and A_{11} have parameters similar as B_7, B_8, B_9, B_{10}, and B_{11}. We only change Taylor-series cosine smooth filter by a wavelet smooth filter with $\omega_t = 0.5, 0.7, 1.2, 1.25, 1.3, 1.6, 1.9, 2.2,$ and 2.32.

From Fig. 8, it can be seen that the Taylor-series cosine smooth filter outperforms the wavelet smooth filter for reducing speckle noise and also NRMS errors in the hologram reconstruction process.

In Fig. 9, we tested the speckle noise when we changed value of ω_t in the wavelet smooth filter and value of ω_0 and ω_1 in the Taylor-series cosine smooth filter. In Fig. 9(a) with screw object and cubic object ω_t change from 0.2 to 2.3.

Fig. 9(b) shows screw object and cubic object; first case: $\omega_0 = 0.2$ is chosen and changing the value of ω_1 when $|\omega_0 - \omega_1| < 1$; second case: $\omega_0 = 1.2$ is chosen and changing value of ω_1 when $1 < |\omega_0 - \omega_1| < 1.5$; third case: $\omega_0 = 1.5$ is chosen and change value of ω_1 when

TABLE 1

Average speckle index of the object reconstruction

	Taylor-series cosine smooth filter	Wavelet smooth filter	Histogram quantization
Speckle index	0.0211	0.0276	0.0353

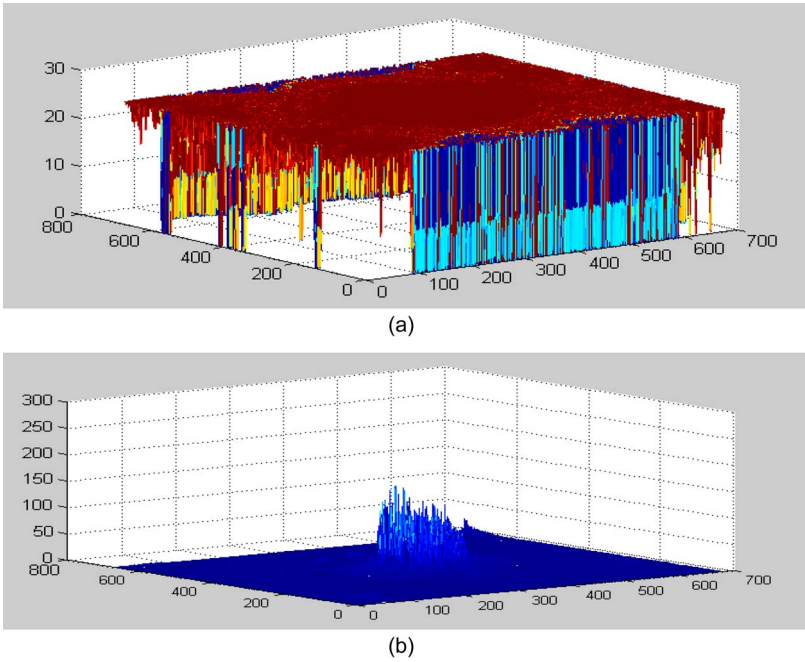

Fig. 12. (a) Noise for reconstructed hologram of cubic object, (b) reconstructed hologram of cubic object after using proposed method with wavelet smooth filter with d = 550 mm.

$1.5 < |\omega_0 - \omega_1| < 2.5$. Both use the Symlet mother wavelet with scales $k = 72$; frequencies sampling is $n = 220$. From this figure, we see that wavelet smooth filter at $\omega_t < 1$ and Taylor-series cosine smooth filter at $\omega_0 = 0.2$, and change value of ω_1 when $|\omega_0 - \omega_1| < 1$ have good result for noise-reducing hologram.

Fig. 10 shows the effect of the size of the small block with speckle index and NRMS errors. For Fig. 10(a) and (b), the cubic object located at 550 mm from the CCD and mother wavelet function is Haar with scales $k = 30$, Daubechies with $n = 3$ and scales $k = 70$, and Symlet with scales $k = 72$.

To evaluate the proposed method with a histogram quantization method at previous research, we calculated the speckle index at different distances, from 240 mm to 900 mm. Fig. 11 shows the speckle index with histogram quantization method with 128 clusters. In Taylor-series cosine smooth case, we use Symlet mother wavelet with scales $k = 72$; frequencies sampling is 220 and is similar with wavelet smooth filter. The average values are shown in Table 1. In the normal low-pass filter, we chose frequencies filter 1.5 and other parameter similar as Taylor-series cosine smooth filter. The improvement of the proposed method with Taylor-cosine smooth filter is 0.0142 and with wavelet smooth filter is 0.0077 compare with the histogram quantization method.

Fig. 12(a) shows the speckle noise is calculated by the proposed method, and Fig. 12(b) shows the cubic object after reconstructing hologram use proposed method that removed speckle noise. From Fig. 12(b), the noise was almost eliminated. Only in the corner of object reconstruction screen,

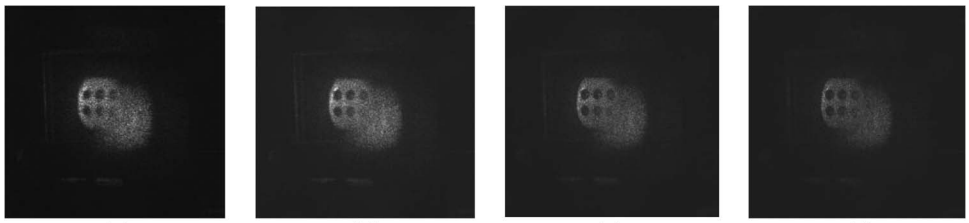

Fig. 13. Hologram reconstruction (a) original, (b) using histogram with 128 clusters; Using the proposed method with (c) wavelet smooth filter, (d) Taylor-series cosine smooth filter.

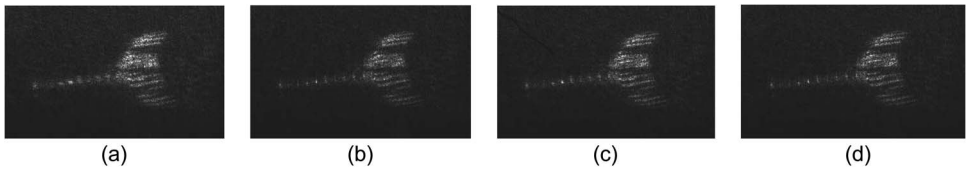

Fig. 14. Hologram reconstruction (a) original, (b) using histogram with 128 clusters; Using the proposed method with (c) wavelet smooth filter, (d) Taylor-series cosine smooth filter.

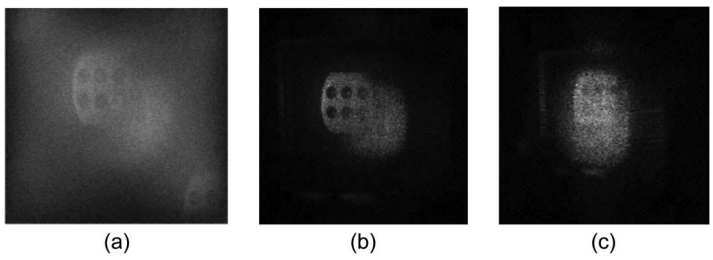

Fig. 15. Hologram reconstruction with normal low-pass filter at distance (a) 250 mm, (b) 530 mm, (c) 980 mm.

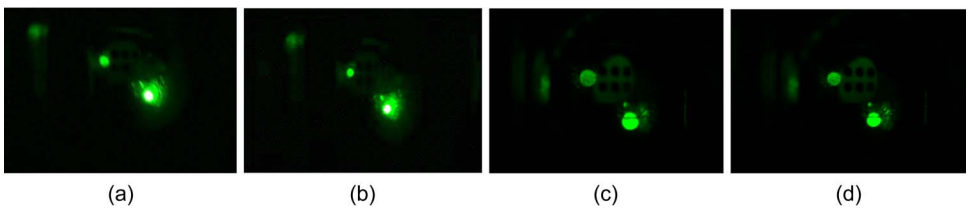

Fig. 16. Hologram reconstruction by SLM with d = 550 mm (a) original, (b) using histogram with 128 clusters; Using the proposed method with (c) wavelet smooth filter, (d) Taylor-series cosine smooth filter.

the noise does not remove due to phase error in the recording process of phase shifting hologram method.

Finally, the above performance analysis was confirmed visually as shown in Figs. 13–17. Figs. 13 and 14 show the cubic object and screw reconstruction by computer with a distance of 550 mm. In Figs. 13 and 14, (a) is original hologram, (b) is hologram reconstruction after using histogram with 128 clusters, (c) is hologram reconstruction after using our proposed method with wavelet smooth filter $\omega_t = 1.5$, and (d) is hologram reconstruction after using our proposed method with Taylor-series cosine smooth filter $\omega_1 = 1,2$ and $\omega_2 = 2.6$, $n = 210$, and size of small block 4×4. It is obvious that the object reconstruction using our proposed method shows less noise than using

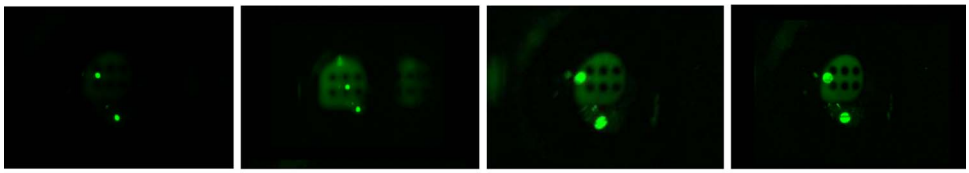

Fig. 17. Hologram reconstruction by SLM with d = 620 mm (a) Original, (b) using histogram with 256 clusters; Using the proposed method with (c) wavelet smooth filter, (d) Taylor-series cosine smooth filter.

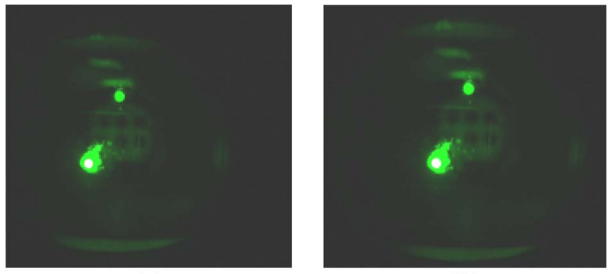

Fig. 18. Hologram reconstruction by SLM d = 900 mm (a) using histogram quantization with 128 clusters, (b) using the proposed method with Taylor-series cosine smooth filter.

histogram quantization with 128 clusters. Fig. 15 has shown the object reconstruction of cubic object with normal low-pass filter at different distances: 250 mm, 530 mm, and 980 mm.

Similarly, Figs. 16 and 17 show the object reconstruction with SLM with a distance of 550 mm and 620 mm by (a) original hologram, (b) using histogram quantization with 128 clusters and 256 clusters, and (c) and (d) using our proposal method with wavelet smooth filter and Taylor-series cosine smooth filter. Finally, effects of different distances are shown in Fig. 18 with distance 900 mm (a) using histogram quantization with 128 clusters and (b) using the proposed method with Taylor-series cosine smooth filter ($\omega_1 = 1, 2$ and $\omega_2 = 2.6$) and Symlet wavelet transform $(k = 70)$. We see that the quality is similarly. Figs. 16–18 confirm the variations of the reconstruction quality according to various parameters that were analyzed above.

5. Conclusion

In this paper, we have proposed a method for noise-reducing created during hologram reconstruction using wavelet transform and a smooth filter. We have also compared the noise-reducing of our proposal with a histogram quantization in hologram reconstruction. From the result of experiments for this algorithm, it showed that the noise-reducing of our proposed method is better than a quantization method. Both simulation and experiments verified the theoretical expectations.

References

[1] L. Pedrotti and L. Frank, *Introduction to Optics*. Englewood Cliffs, NJ, USA: Prentice-Hall, 1993, pp. 96–120.
[2] M. Gross, M. Atlan, and E. Absil, "Noise and aliases in off-axis and phase-shifting holography," *Appl. Opt.*, vol. 47, no. 11, pp. 1757–1766, Apr. 2008.
[3] F. Nicolas, S. Coetmellec, M. Brunel, and D. Lebrun, "Digital in-line holography with a sub-picosecond laser beam," *Opt. Commun.*, vol. 268, no. 1, pp. 27–33, Dec. 2006.
[4] T. Kreis, W. Juptner, and J. Geladmacher, "Principles of digital holographic interferometry," *Proc. SPIE*, vol. 3478, pp. 45–48, Jun. 1988.
[5] E. Cuche, P. Marquet, and C. Depeursinge, "Spatial filtering for zero-order and twin-image elimination in digital off-axis holography," *Appl. Opt.*, vol. 39, no. 23, pp. 4070–4075, Aug. 2000.

[6] Y. Pu and H. Meng, "Intrinsic speckle noise in off-axis particle holography," *J. Opt. Soc. Amer. A*, vol. 21, pp. 1221–1230, Jul. 2004.
[7] I. Yamaguchi, "Phase-shifting digital holography," *Opt. Lett.*, vol. 22, no. 16, pp. 1268–1270, Aug. 1997.
[8] A. Sharma, G. Sheoran, and A. Jaffery, "Improvement of signal-to-noise ratio in digital holography using wavelet transform," *Opt. Laser Eng.*, vol. 46, pp. 42–47, Jan. 2008.
[9] E. Darakis and J. Soraghan, "Use of Fresnelets for phase-shifting digital hologram compression," *IEEE Trans. Image Process.*, vol. 15, no. 12, pp. 3804–3811, Dec. 2006.
[10] W. Dallas and A. Lohmann, "Phase quantization in holograms-depth effects," *Appl. Opt.*, vol. 11, no. 1, pp. 192–194, Jan. 1972.
[11] A. Shortt, T. Naughton, and B. Javidi, "A companding approach for nonuniform quantization of digital hologram of three-dimensional objects," *Opt. Exp.*, vol. 14, no. 12, pp. 5219–5134, Jun. 2006.
[12] V. Kober, L. Yaroslavsky, J. Campos, and M. Yzuel, "Optimal filter approximation by means of a phase-only filter with quantization," *Opt. Lett.*, vol. 19, no. 13, pp. 978–980, Jul. 1994.
[13] A. Shortt, T. Naughton, and B. Javidi, "Histogram approaches for lossy compression of digital hologram of three-dimensional objects," *IEEE Trans. Image Process.*, vol. 16, no. 6, pp. 1548–1556, Jun. 2007.
[14] L. Bang, Z. Ali, P. Quang, J. Park, and N. Kim, "Compression of digital hologram for three-dimensional object using wavelet-bandelets transform," *Opt. Exp.*, vol. 19, no. 9, pp. 8019–8031, Apr. 2011.
[15] Y. Linde, A. Buzo, and R. Gray, "An algorithm for vector quantizer design," *IEEE Trans. Commun.*, vol. COM-28, no. 1, pp. 84–95, Jan. 1980.
[16] N. Gallagher, "Optimum quantization in digital holography," *Appl. Opt.*, vol. 17, no. 1, pp. 109–115, Jan. 1978.
[17] H. Choi, Y. Seo, and D. Kim, "Noise reduction for digital holograms in a discrete cosine transform (DCT) domain," *Optic. Appl.*, vol. 40, no. 4, pp. 991–1005, Dec. 2010.
[18] E. Ribak, C. Roddier, F. Roddier, and B. Breckinridge, "Signal-to-noise limitation in white light holography," *Appl. Opt.*, vol. 27, no. 6, pp. 1183–1186, Mar. 1988.
[19] M. Pilkington and W. Roest, "Draping aeromagnetic data in areas of rugged topography," *J. Appl. Geophys.*, vol. 29, no. 2, pp. 135–142, Aug. 1992.
[20] M. Vetterli and C. Herley, "Wavelets and filter banks: Theory and design," *IEEE Trans. Signal Process.*, vol. 40, no. 9, pp. 2207–2232, Sep. 1992.
[21] J. Goodman, *Introduction to Fourier Optics*. New York, USA: McGraw-Hill, 1996, pp. 32–55.
[22] G. Mills and I. Yamaguchi, "Effects of quantization in phase-shifting digital holography," *Appl. Opt.*, vol. 44, no. 7, pp. 1216–1225, Mar. 2005.
[23] B. Javidi and E. Tajahuerce, "Three-dimensional object recognition by use of digital holography," *Opt. Lett.*, vol. 25, no. 9, pp. 610–612, May 2000.
[24] G. Kaiser, "Wavelet filtering in the scale domain," *Proc. SPIE*, vol. 2825, pp. 226–237, Oct. 1996.
[25] A. Antoniou, *Digital Filters: Analysis Design and Applications*. New York, USA: McGraw-Hill, 1993, pp. 541–600.
[26] I. Khan and R. Ohba, "New design of full band differentiators based on Taylor series," *IEEE Proc.-Vis. Image Signal Process.*, vol. 146, no. 4, pp. 185–189, Aug. 1999.
[27] G. Strang, *Linear Algebra and Its Applications*. Pacific Grove, CA, USA: Brooks/Cole, 1988.
[28] S. Mirza, R. Kumar, and C. Shaker, "Reduction of speckle noise in digital holographic images using wavelet transform," *Proc. SPIE*, vol. 7155, pp. 51–58, Oct. 2008.
[29] Y. Chung, I. Matsubara, and W. Dallas, "Speckle noise reduction for digital holography using longitudinal shifting," presented at the Proc. Digital Holography Three-Dimensional Imaging (DH), Miami, FL, USA, Apr.28, 2012, DM4C.4.
[30] R. Crimmins, "Geometric filter for speckle reduction," *Appl. Opt.*, vol. 24, no. 10, pp. 1438–1443, May 1985.